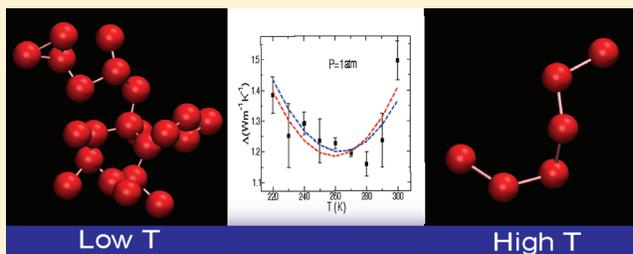# Thermal Conductivity Minimum: A New Water Anomaly

Pradeep Kumar*,[†] and H. Eugene Stanley[‡]

[†]Center for Studies in Physics and Biology, 1230 York Avenue, Rockefeller University, New York, New York 10021, United States
[‡]Center for Polymer Studies and Department of Physics, Boston University, Boston, Massachusetts 02215, United States

ABSTRACT: We investigate the thermal conductivity of liquid water using computer simulations of the TIP5P model of water. Our simulations show that, in addition to the maximum at high temperatures at constant pressure that it exhibits in experiments, the thermal conductivity also displays a minimum at low temperatures. We find that the temperature of minimum thermal conductivity in supercooled liquid water coincides with the temperature of maximum specific heat. We discuss our results in the context of structural changes in liquid water at low temperatures.

I. INTRODUCTION

For a number of decades, the anomalous behavior of water, e.g., the increase of density upon heating and the increase of diffusivity upon compression, has been the subject of intense research.[1-7] More than 80 anomalies of water have been discovered in experiments. Some of these anomalies concern static thermodynamic properties, e.g., the increase of compressibility and specific heat when the temperature is decreased, and others concern dynamic properties, e.g., the breakdown of the Stokes–Einstein relation[8,9] and the non-Arrhenius to Arrhenius dynamic crossover at low temperatures.[9-11]

To explain the anomalous behavior of water, the existence of a liquid–liquid (LL) phase transition has been proposed,[12,13] but this hypothesized LL transition lies in a region of the pressure–temperature phase diagram inaccessible to experimentation on bulk water due to crystallization of the liquid within experimental time scales. Fortunately, the crystallization within this temperature region occurs at microsecond time scales, but the density relaxation of liquid is in the range of tens of nanoseconds (Figure 1). Thus, because of this rapid relaxation time, it is possible to study the metastable equilibrium behavior of liquid water at low temperatures using computer simulation.[12,14-16]

Recent neutron scattering studies of liquid water by the groups of S.-H. Chen and F. Mallamace[8,17-20] support the possible existence of a first-order phase transition in liquid water that ends at a liquid–liquid critical point.[9,10,21] By confining water in MCM-41, a matrix of hexagonal silica pores, Chen and his colleagues were able to measure the density relaxation time of confined water at temperatures as low as $T = 180$ K. In their experiments, they found that water undergoes a dynamic crossover at $T \approx 225$ K, where the dynamics change from non-Arrhenius at high temperatures to Arrhenius at low temperatures. Subsequent studies of different molecular and coarse-grained models suggest that the observed dynamic crossover occurs when the line of maximum correlation length is crossed due to decreasing temperatures.[10,11,21] Specifically, it was shown that, as the temperature is decreased at a constant

pressure (a pressure lower than the LL-critical pressure), the system crosses the line of correlation length maximum emanating from the hypothesized LL-critical point into the supercritical one-phase liquid regime. This line, designated the Widom line $T_W(P,T)$,[10,21-23] is associated with a sharp but continuous change in the value of the local order of the liquid which, in turn, induces a sharp but continuous change in the strength of entropy and entropy fluctuations, leading to a maximum in the specific heat.[10,23]

When the Widom line is crossed, many of the physical properties of liquid water change. The physical properties of liquid water resemble the properties of a high density liquid at high temperatures and a low density liquid at temperatures below T_W.[10,23] While the thermal conductivity of water is experimentally measurable down to temperatures just below the melting point,[24] the thermal diffusion in the deeply supercooled regime is still unknown. The known experimental values of the thermal conductivity display a nonmonotonic behavior as a function of temperature at atmospheric pressure.[24] Moreover, the thermal conductivity decreases when the temperature drops below the melting point. It is not clear whether the thermal conductivity would decrease upon a further decrease of temperature. In this paper, we study heat conduction in liquid water over a wide range of temperatures using computer simulations of the TIP5P model.[25,26]

II. SIMULATION METHODS

In our investigation of the thermal diffusivity of water, we perform computer simulations using the TIP5P model over a wide range of temperatures and atmospheric pressure.[25-28] The TIP5P model is able to reproduce the qualitative behavior of liquid water over a broad region of the phase diagram. The details of the interactions

14269   dx.doi.org/10.1021/jp2051867 | *J. Phys. Chem. B* 2011, 115, 14269–14273
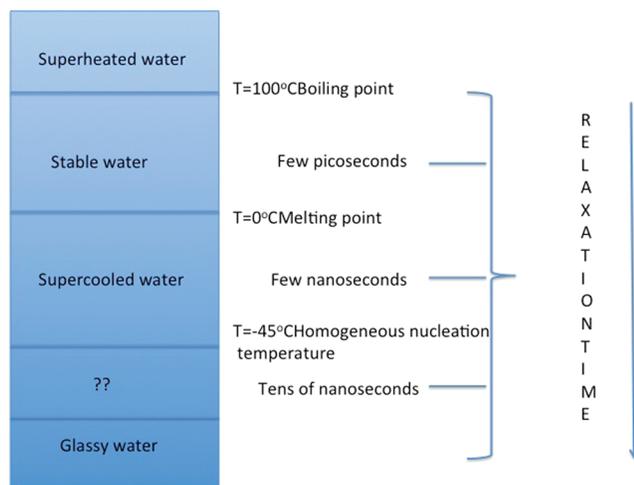
Figure 1. Schematic of the phase diagram of water at atmospheric pressure. The density relaxation time of liquid water increases with decreasing temperature.
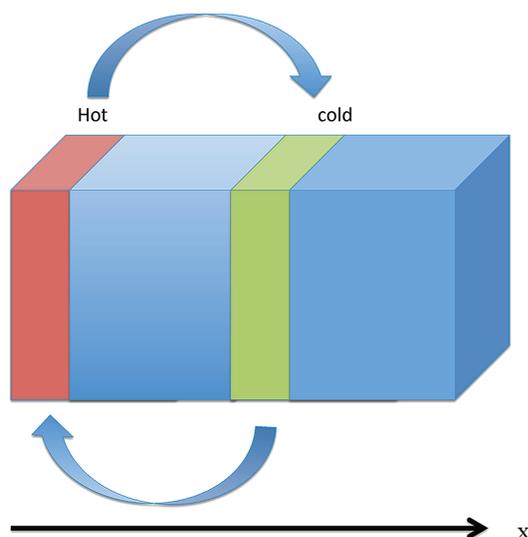

Figure 2. To use the MP algorithm to calculate the thermal conductivity, the simulation box was divided into $N_{slab} = 12$ slabs along the x direction. The first and central slabs were then chosen as the hot and cold regions, respectively, for swapping molecules.

and simulations are discussed in refs 9 and 25. All the calculations of thermal conductivity were done using the NVE ensemble.

A. Computation of Thermal Conductivity. We use Muller−Plathe (MP) methods[29] to compute the thermal conductivity of water at different temperatures. There are several other methods of computing the thermal conductivity of a liquid, e.g., using the heat current correlation function with the Green−Kubo formula[30] or using nonequilibrium molecular dynamics. The current correlation function approach is direct and can be determined using equilibrium simulations. It allows us to compute the integral of the heat current correlation function but suffers from poor convergence even for extremely long simulations. It has been shown in earlier studies of both simple and molecular liquids[31,32] that the MP method not only gives reasonably accurate thermal conductivity but it also produces an acceptable convergence and is easy to implement.[29] Thus, we chose the MP method for our computations.
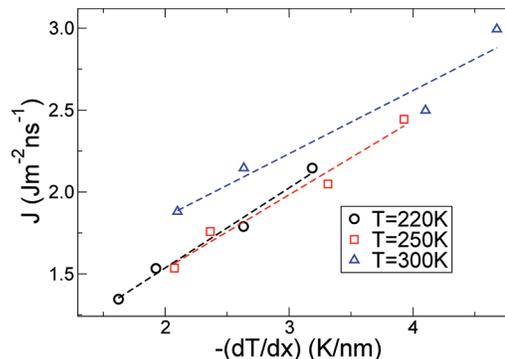

Figure 3. Heat flux J for three different temperatures as a function of the temperature gradient $-(\langle \partial T/\partial x \rangle)$. Dashed lines are linear fits through the data, suggesting a linear regime at these flux values.
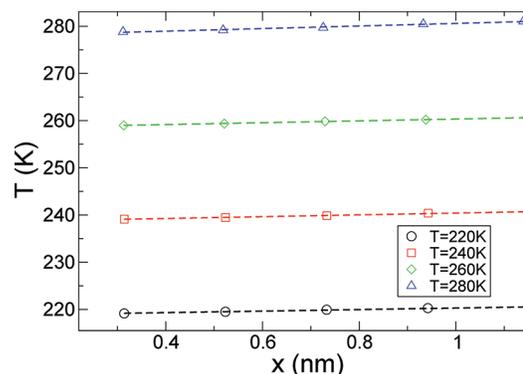

Figure 4. Average temperature T as a function of distance from the cold slab used to calculate $\langle \partial T/\partial x \rangle$. The x values are the midpoints of the intervening slabs between the hot and cold slabs.

B. The Muller−Plathe (MP) Algorithm. We use the algorithm described in ref 29 to calculate the thermal conductivity of liquid water at a number of different temperatures. We divide the simulation box in the x-direction into 12 slabs (Figure 2). The average temperature gradient $\langle \partial T/\partial x \rangle$ between the hot and cold slabs is determined by swapping the velocities of the fastest water molecule in the cold slab with the slowest molecule in the hot slab, as described in ref 29. $\langle \partial T/\partial x \rangle$ reaches a constant value in 10−20 ns, depending on the temperature. Note that this method conserves both the momentum and the energy of the system, since, although the velocities are swapped, the configuration remains unchanged. We first compute the temperature gradient $\langle \partial T/\partial x \rangle$ for different swap rates and hence different heat flux values at a given temperature. For small swap rates (small flux), we find that the system is within the linear regime and the heat flux J can be determined using Fourier's law of heat conduction

$$J = -\Lambda \left\langle \frac{\partial T}{\partial x} \right\rangle \tag{1}$$

where $\langle \partial T/\partial x \rangle$ is the average temperature gradient, Λ is the thermal conductivity, and J is the total flux given by

$$J = \frac{1}{2 L_y L_z t} \sum_{swaps} \frac{1}{2} [m(v_h^2 - v_c^2)] \tag{2}$$

where the sum is taken over all the swaps in a given time t and v_h and v_c are the velocities of the cold and hot molecules being swapped. Once

we are sure that the flux is small enough for the system to be within the linear regime, we calculate Λ by calculating $\langle \partial T/\partial x \rangle$ in the case of the smallest flux and using eq 1. The error bars on the values of Λ are obtained using the linear propagation of errors in eq 1, which gives the error $\Delta\Lambda = J\Delta\langle \partial T/\partial x \rangle/(\langle \partial T/\partial x \rangle)^2$.

III. RESULTS

Figure 3 shows the heat flux J as a function of gradient for various temperatures. For a small flux (or small swap rate), J is a linear function of temperature gradient $\partial T/\partial x$. At small values of the heat flux, the temperature gradient is typically of the order of 2–3 K/nm, which is a small perturbation to the system about equilibrium. Figure 4 shows the temperature T along the molecule swap direction. A convergence of the temperature profile is obtained within a range of 10–20 ns, depending on the temperature. From the slope, we calculate $\langle \partial T/\partial x \rangle$ and thermal conductivity Λ.

Figure 5a shows the values of thermal conductivity Λ as a function of temperature for pressure $P = 1$ atm below the liquid–liquid critical pressure for the TIP5P model. We also show quadratic fits to the data (dashed lines). Λ decreases upon decreasing temperature, an experimental behavior of liquid water down to 265 K.[24] However, upon a further decrease of T, Λ reaches a minimum at low temperature $T_{min}^{\Lambda} \approx 255$ K, below which it increases. A clue to the possible interpretation of this surprising result is that the temperature at which Λ displays a minimum is approximately the same as the temperature at which the specific heat C_P displays a maximum (see Figure 5b).

Finally, we calculate the thermal diffusivity D_T, which is related to ρ and C_P as $D_T = \Lambda/\rho C_P$. Figure 5c shows that D_T decreases very slowly with decreasing T and then rises sharply when T drops below the temperature of maximum C_P.

Note that a maximum in C_P occurs upon crossing the locus of maximum correlation length—the Widom line $T_W(P,T)$—emanating from the hypothesized liquid–liquid critical point.[10] Below $T_W(P,T)$, liquid water becomes locally more tetrahedral[21] and its structure resembles the structure of ice Ih. The thermal conductivity value of ice Ih at the melting point $T = 273.15$ K is ≈ 2.14 W m^{-1} K^{-1},[33] while the thermal conductivity of liquid water at $T = 275$ K is 0.56 W m^{-1} K^{-1}.[24] Moreover, the thermal conductivity of ice increases upon decreasing temperature. We hypothesize that the increase in thermal conductivity of supercooled water at low temperatures occurs because of the structural changes in water at T_W.

To test our hypothesis, we calculate the average cluster size of molecules with large tetrahedral order parameter Q,[34] defined for molecule k as

$$Q_k = 1 - \frac{3}{8}\sum_i \sum_{j>i}\left[\cos(\Psi_{ikj}) + \frac{1}{3}\right]^2 \qquad (3)$$

where Ψ_{ikj} is the angle between central molecule k and neighbors i and j in the nearest neighbor shell. It has been shown that the distribution of the local tetrahedral order parameter shows a bimodal behavior at high T and changes to unimodal at low T.[23] To make a distinction between ordered and disordered molecules, we choose a cutoff value Q_c and assume that any molecule with $Q > Q_c$ is an ordered molecule. We also assume that two ordered molecules i and j with $r_{ij} < 0.35$ belong to the same cluster.
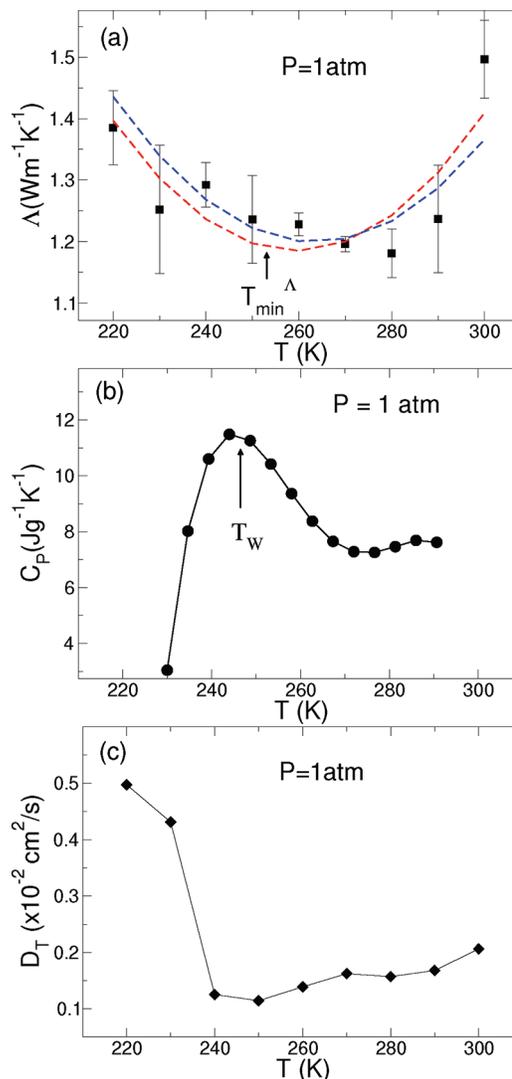

Figure 5. (a) Thermal conductivity Λ (solid squares) as a function of T at atmospheric pressure showing a minimum at $T \approx 255$ K. Errors in Λ are estimated by using the linear propagation of errors in eq 1. The dashed red curve is a quadratic fit to the data without weighting the errors, while the dashed blue curve is a quadratic weighted fit to the data using the weight function $1/(\Delta\Lambda)^2$. (b) Isobaric heat capacity C_P as a function T showing a maximum at $T \approx 250$ K. (c) Thermal diffusivity D_T showing a sharp jump below $T \approx 250$ K.

Figure 6 shows the temperature dependence of the cluster size distribution $P(s)$ for $P = 1$ atm. We find that, for the range of temperatures studied, $P(s)$ follows an exponential distribution. Moreover, at high T, cluster size s is small with very few molecules participating in the ordered cluster. As the temperature is decreased, the cluster size grows, and this is reflected in the large decay constant of the exponential at low T. Furthermore, the cluster size distribution at low T shows an exponential behavior at small values of s but deviates from exponential behavior at large values of s. This may be due to the small system size or the bad convergence of $P(s)$, since the probability of large clusters developing is small. At the lowest studied temperature, the cluster size found in our simulations could be as high as 30–40 molecules.

Our results suggest that the reversal of the behavior of thermal conductivity is related to the onset of large clusters of ordered
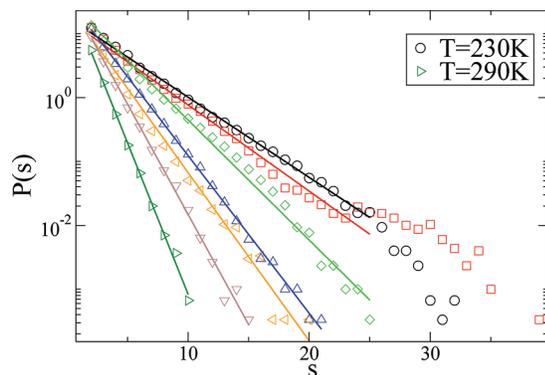
Figure 6. Histogram $P(s)$ of cluster size s of molecules with a high degree of tetrahedrality for various temperatures at atmospheric pressure. $P(s)$ follows an exponential distribution at all T with decay constant decreasing monotonically with decreasing temperature.

water molecules below T_W. A similar increase in the thermal conductivity upon ordering has been observed in other systems.[35] In order to understand why the heat conduction increases at low temperatures, we must understand how the structure of liquid water causes changes in phonon modes. Furthermore, neutron scattering experiments[8] reveal an onset of low frequency dispersionless excitations in hydration water below T_W.[36] In order to better understand the behavior of thermal conductivity at low temperatures, further study of the nature of phonons and these low-frequency excitations is needed.[36]

IV. DISCUSSION AND SUMMARY

We have studied the thermal conductivity of liquid water in the deep supercooled regime and have found that the thermal conductivity decreases upon lowering the temperature but reverses its behavior below T_{min}^Λ, where it increases upon a further decrease of temperature. The temperature of minimum thermal conductivity T_{min}^Λ coincides with the temperature of maximum specific heat. We hypothesize that the increase of thermal conductivity at low temperatures is due to an ordering of the tetrahedral network of water molecules, a structural picture consistent with the hypothesized liquid−liquid phase transition and its associated Widom line.[10,21] To further test our hypothesis, we calculate the cluster sizes of ordered tetrahedral molecules at different temperatures and find that the distribution of cluster sizes follows an exponential behavior that changes sharply at the Widom temperature.

Although our results are calculated for a small system, $N = 512$, the thermal conductivity decrease with decreasing temperature agrees qualitatively with experimental data down to 265 K. The model also displays an experimentally known maximum in thermal conductivity at high temperatures. We note that, at lower temperatures as the correlation length of the system increases, a system-size-dependent study of thermal conductivity will be necessary. Moreover, in order to precisely understand the nature of this increase in Λ, further studies of phonons and the onset of low frequency excitations in water at low temperatures will be needed.

■ ACKNOWLEDGMENT

■ REFERENCES

(1) Stanley, H. E.; Buldyrev, S. V.; Kumar, P.; et al. *J. Non-Cryst. Solids* **2009**, *357*, 629–640.

(2) Debenedetti, P. G.; Stanley, H. E. *Phys. Today* **2003**, *56* (6), 40–46.

(3) Debenedetti, P. G. *J. Phys.: Condens. Matter* **2003**, *15*, R1669–R1726.

(4) Angell, C. A. *Annu. Rev. Phys. Chem.* **2004**, *55*, 559–583.

(5) Buldyrev, S. V.; Kumar, P.; Debenedetti, P. G.; et al. *Proc. Natl. Acad. Sci. U.S.A.* **2007**, *104*, 20177–20182.

(6) Han, S.; Choi, M. Y.; Kumar, P. *Nat. Phys.* **2010**, 685–689.

(7) Kumar, P.; Sungho, Han; Stanley, H. E. *J. Phys.: Condens. Matter* **2009**, *21*, 504108.

(8) Chen, S.-H.; Mallamace, F.; Mou, C.-Y; Broccio, M.; Corsaro, C.; Faraone, A.; Liu, L. *Proc. Natl. Acad. Sci. U.S.A.* **2006**, *103*, 12974–12978. Kumar, P. *Proc. Natl. Acad. Sci. U.S.A.* **2006**, *103*, 12955–12956.

(9) Kumar, P.; Buldyrev, S. V.; Becker, S. R.; Poole, P. H.; Starr, F. W.; Stanley, H. E. *Proc. Natl. Acad. Sci. U.S.A.* **2007**, *103*, 9575–9579.

(10) Xu, L.; Kumar, P.; Buldyrev, S. V.; Chen, S.-H.; Poole, P.; Sciortino, F.; Stanley, H. E. *Proc. Natl. Acad. Sci. U.S.A.* **2005**, *102*, 16558–16562.

(11) Kumar, P.; Franzese, G.; Stanley, H. E. *Phys. Rev. Lett.* **2008**, *100*, 105701[1−4].

(12) Poole, P. H.; Sciortino, F.; Essmann, U.; Stanley, H. E. *Nature* **1992**, *360*, 324–328.

(13) Mishima, O.; Stanley, H. E. *Nature* **1998**, *392*, 164–168.

(14) Starr, F. W.; Angell, C. A.; Stanley, H. E. *Physica A* **2003**, *323*, 51–66.

(15) Poole, P. H.; Saika-Voivod, I.; Sciortino, F. *J. Phys.: Condens. Matter* **2005**, *17*, L431–L437.

(16) Sastry, S.; Sciortino, F.; Stanley, H. E. *J. Chem. Phys.* **1991**, *95*, 7775–7776.

(17) Liu, L.; Chen, S.-H.; Faraone, A.; Yen, C.-W.; Mou, C.-Y. *Phys. Rev. Lett.* **2005**, *95*, 117802[1−4].

(18) Mallamace, F.; Broccio, M.; Corsaro, C.; Faraone, A.; Wanderlingh, U.; Liu, L.; Mou, C.-Y.; Chen, S.-H. *J. Chem. Phys.* **2006**, *124*, 161102 [1−4].

(19) Faraone, A.; Liu, L.; Mou, C.-Y; Yen, C.-W.; Chen, S.-H. *J. Chem. Phys.* **2004**, *121*, 10843–10846.

(20) Zhang, Y.; Faraone, A.; Kamitakahara, W. A.; Liu, K.-H.; Mou, C.-Y.; Leão, J. B.; Chang, S.; Chen, S.-H. *Proc. Natl. Acad. Sci. U.S.A.* **2011**, *108*, 12206–12211.

(21) Kumar, P.; Yan, Z.; Xu, L.; Mazza, M.; Buldyrev, S. V.; Chen, S.-H.; Sastry, S.; Stanley, H. E. *Phys. Rev. Lett.* **2006**, *97*, 177802[1−4].

(22) Anisimov, M. A.; Sengers, J. V.; Levelt Sengers, J. M. H. In *Aqueous System at Elevated Temperatures and Pressures: Physical Chemistry in Water, Stream and Hydrothermal Solutions*; Palmer, D. A., Fernandez-Prini, R., Harvey, A. H., Eds.; Elsevier: Amsterdam, The Netherlands, 2004.

(23) Kumar, P.; Buldyrev, S. V.; Stanley, H. E. *Proc. Natl. Acad. Sci. U.S.A.* **2009**, *106*, 22130–22134.

(24) IAPWS Release on the *Thermal Conductivity of Ordinary Water Substance*, IAPWS Secretariat 1998.

(25) Mahoney, M. W.; Jorgensen, W. L. *J. Chem. Phys.* **2000**, *112*, 8910–8922.

(26) Yamada, M.; Mossa, S.; Stanley, H. E.; Sciortino, F. *Phys. Rev. Lett.* **2002**, *88*, 195701[1−4].

(27) Paschek, D. *Phys. Rev. Lett.* **2005**, *94*, 217802[1−4].

(28) Kumar, P.; Buldyrev, S. V.; Stanley, H. E. Dynamic Crossover and Liquid-Liquid Critical Point in the TIP5P Model of Water. In *Soft Matter under Extreme Pressures: Fundamentals and Emerging Technologies*; Rzoska, S. J., Mazur, V., Eds.; Proc. NATO ARW, Odessa, Oct 2005; Springer: Berlin, 2006.

(29) Müller-Plathe, F. *J. Chem. Phys.* **1997**, *106*, 6082–6085.

(30) Green, M. S. *J. Chem. Phys.* **1957**, *22*, 398–413. Kubo, R. *J. Phys. Soc. Jpn.* **1957**, *12*, 570–586.

(31) Nieto-Draghi, C.; et al. *J. Chem. Phys.* **2007**, *126*, 064509.

14272

dx.doi.org/10.1021/jp2051867 |*J. Phys. Chem. B* 2011, 115, 14269–14273

(32) Stackhouse, S.; Stixrude, L.; Kirki, B. B. *Phys. Rev. Lett.* **2010**, *104*, 208501[1−4].

(33) Slack, G. A. *Phys. Rev. B* **1980**, *22*, 3065−3071.

(34) Errington, J. R.; Debenedetti, P. G. *Nature (London)* **2001**, *409*, 318−321.

(35) Févere, M.; Finel, A.; Caudron, R.; Mevrel, R. *Phys. Rev. B* **2005**, *72*, 104118[1−4].

(36) Kumar, P.; Wikfeldt, T.; Schlesinger, D.; Pettersson, L. G. M.; Stanley, H. E. (preprint).

(37) Das, S. K. et al. *Phys. Rev. Lett.* **2006**; *97*, 025702; *J. Chem. Phys.* **2006**, *125*, 024506; *J. Chem. Phys.* **2007**, *127*, 144506.

■ NOTE ADDED IN PROOF

After the completion of this work, we were made aware of interesting works relevant to finite-size effects on the evaluation of transport properties.[37]

14273

dx.doi.org/10.1021/jp2051867 |*J. Phys. Chem. B* 2011, 115, 14269–14273